Title	A tunable microwave slot antenna based on graphene
Authors	Dragoman, Mircea;Neculoiu, Dan;Bunea, Alina-Cristina;Deligeorgis, George;Aldrigo, Martino;Vasilache, Dan;Dinescu, Adrian;Konstantinidis, George;Mencarelli, Davide;Pierantoni, Luca;Modreanu, Mircea
Publication date	2015
Original Citation	Dragoman, M., Neculoiu, D., Bunea, A.-C., Deligeorgis, G., Aldrigo, M., Vasilache, D., Dinescu, A., Konstantinidis, G., Mencarelli, D., Pierantoni, L. and Modreanu, M. (2015) 'A tunable microwave slot antenna based on graphene', Applied Physics Letters, 106(15), pp. 153101. doi: 10.1063/1.4917564
Type of publication	Article (peer-reviewed)
Link to publisher's version	http://aip.scitation.org/doi/abs/10.1063/1.4917564 - 10.1063/1.4917564
Rights	© 2015 AIP Publishing LLC. This article may be downloaded for personal use only. Any other use requires prior permission of the author and AIP Publishing. The following article appeared in Dragoman, M., Neculoiu, D., Bunea, A.-C., Deligeorgis, G., Aldrigo, M., Vasilache, D., Dinescu, A., Konstantinidis, G., Mencarelli, D., Pierantoni, L. and Modreanu, M. (2015) 'A tunable microwave slot antenna based on graphene', Applied Physics Letters, 106(15), pp. 153101 and may be found at http://aip.scitation.org/doi/abs/10.1063/1.4917564.
Download date	2024-07-11 19:21:44
Item downloaded from	https://hdl.handle.net/10468/4252

University College Cork, Ireland
Coláiste na hOllscoile Corcaigh

A tunable microwave slot antenna based on graphene

Mircea Dragoman, Dan Neculoiu, Alina-Cristina Bunea' , George Deligeorgis, Martino Aldrigo, D. Vasilache, A. Dinescu, George Konstantinidis, Davide Mencarelli, Luca Pierantoni, and M. Modreanu

Citation: Appl. Phys. Lett. **106**, 153101 (2015); doi: 10.1063/1.4917564
View online: http://dx.doi.org/10.1063/1.4917564
View Table of Contents: http://aip.scitation.org/toc/apl/106/15
Published by the American Institute of Physics

A tunable microwave slot antenna based on graphene

Mircea Dragoman,[1] Dan Neculoiu,[1,2] Alina-Cristina Bunea,[1,2,a)] George Deligeorgis,[3] Martino Aldrigo,[1] D. Vasilache,[1] A. Dinescu,[1] George Konstantinidis,[3] Davide Mencarelli,[4] Luca Pierantoni,[4] and M. Modreanu[5]
[1]*National Institute for Research and Development in Microtechnology (IMT), Str. Erou Iancu Nicolae 126 A, 077190 Bucharest-Voluntari, Romania*
[2]*"Politehnica" University of Bucharest, Bd. Iuliu Maniu 1-3, 061071, Bucharest, Romania*
[3]*Foundation for Research and Technology Hellas (FORTH), P.O. Box 1527, Vassilika Vuton, Heraklion 71110, Crete, Hellas, Greece*
[4]*Università Politecnica delle Marche, via Brecce Bianche 12, 60131 Ancona, Italy*
[5]*Tyndall National Institute, Lee Maltings Complex, Dyke Parade, Cork, Ireland*

(Received 20 March 2015; accepted 3 April 2015; published online 13 April 2015)

The paper presents the experimental and modeling results of a microwave slot antenna in a coplanar configuration based on graphene. The antennas are fabricated on a 4 in. high-resistivity Si wafer, with a ~300 nm SiO_2 layer grown through thermal oxidation. A CVD grown graphene layer is transferred on the SiO_2. The paper shows that the reflection parameter of the antenna can be tuned by a DC voltage. 2D radiation patterns at various frequencies in the X band (8–12 GHz) are then presented using as antenna backside a microwave absorbent and a metalized surface. Although the radiation efficiency is lower than a metallic antenna, the graphene antenna is a wide-band antenna while the metal antennas with the same geometry and working at the same frequencies are narrowband. © *2015 AIP Publishing LLC*. [http://dx.doi.org/10.1063/1.4917564]

Various physical phenomena, which are key concepts in applied physics, are studied with the mono- and multilayer graphene in the high frequencies, especially in microwave frequencies. We mention here briefly Faraday rotation,[1] localization and antilocalization,[2] optomechanics phenomena and detection of mechanical quanta,[3] optomechanical coupling of graphene mechanical resonators and superconducting cavities,[4] quantum oscillations at microwaves frequencies,[5] and time flow in graphene.[6]

Also, the graphene monolayer plays an increased role in high frequency electronics including terahertz (THz) frequency range. A series of innovative high frequency devices based on graphene have been fabricated and measured boosting graphene electronics up to THz.

Few examples are graphene field-effect transistors (FETs) with $f_{max} = 70$ GHz,[7] graphene FETs with cutoff frequencies in the THz range,[8,9] microwave and millimeter wave generation via multiplication,[10] even graphene receivers at microwave frequencies,[11,12] and THz frequencies.[13,14]

The antennas are key components in any wireless communication system. In the perspective of integrated circuits at high frequencies,[11] the antenna integrated with the other graphene devices on the same chip is an immediate demand.

Therefore, it is interesting to study a microwave antenna based on graphene and its properties. The main obstacle up to now to study passive microwave devices based on graphene is that the wavelengths in the microwave range (between 10 and 100 mm) are much larger than the graphene flakes (with dimensions of few millimeters). However, the CVD growth of graphene and its transfer on various substrates, especially onto Si/SiO_2, has attained impressive performances in few years. Nowadays, batch production of graphene monolayer is performed at 4-in. and 6-in. wafer scale; 12-in. wafers are being expected in only a few years.[15]

What can we expect from passive devices including antennas based on graphene? The surface impedance of a graphene monolayer is given by $Z_S(V_b) = 1/\sigma(\omega) = R_s(V_b) + jX_s(V_b)$, where $\sigma(\omega)$ is the graphene conductivity and V_b is the DC applied voltage. Since $\sigma(\omega)$ is dependent on a DC voltage applied vertically either as top gate and/or back-gate voltage as in the case of graphene transistors or as a tangential field across a slot as in the case of graphene coplanar waveguides,[16] the tunability of microwave S-parameters by means of the applied voltage is obtained, which is a great advantage. Up to now, only ferromagnetic, ferroelectric, and liquid crystals have conferred an inherent tunability of the microwave devices.[17] However, in the microwave range, the surface resistance is, in principle, greater than a few hundreds of ohms when no bias is applied, which is a detrimental effect implying losses and moderate radiation efficiencies.

The fabricated microwave antenna is displayed in Figs. 1(a) and 1(b). We can see that the antenna is fabricated in coplanar waveguide topology, and the rectangular patch is made from graphene and separated by a slot from the rest of the circuit, which is made from gold. The outer gold electrodes are grounded while the central electrode is excited by the microwave signal. The main dimensions of the antenna are depicted in Fig. 1(c).

Several graphene-based antennas were fabricated on the same wafer with commercially grown and transferred graphene by Graphenea. The 4 in. high resistivity Si wafer has a thickness of 500 μm with a 300 nm SiO_2 layer grown through thermal oxidation. Micro-Raman spectra in the region of the microwave graphene-based antenna have been aquired in 180° backscattering configuration using a InVia Reflex

a)Author to whom correspondence should be addressed. Electronic mail: alina.bunea@imt.ro

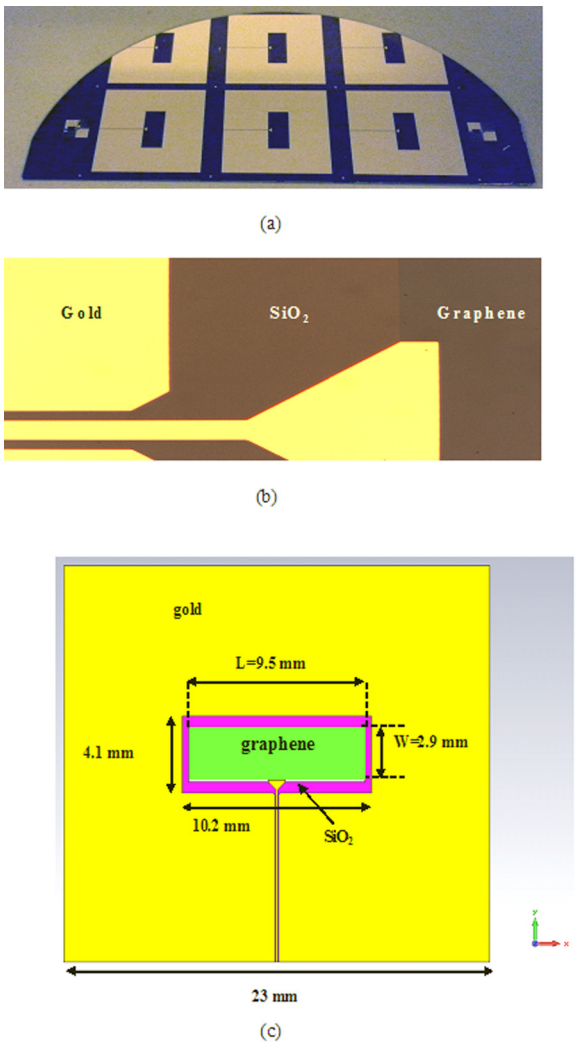

FIG. 1. The microwave graphene antenna: (a) optical image of the fabricated graphene based antennas, (b) detailed view of the graphene/gold interface, and (c) layout with final dimensions.

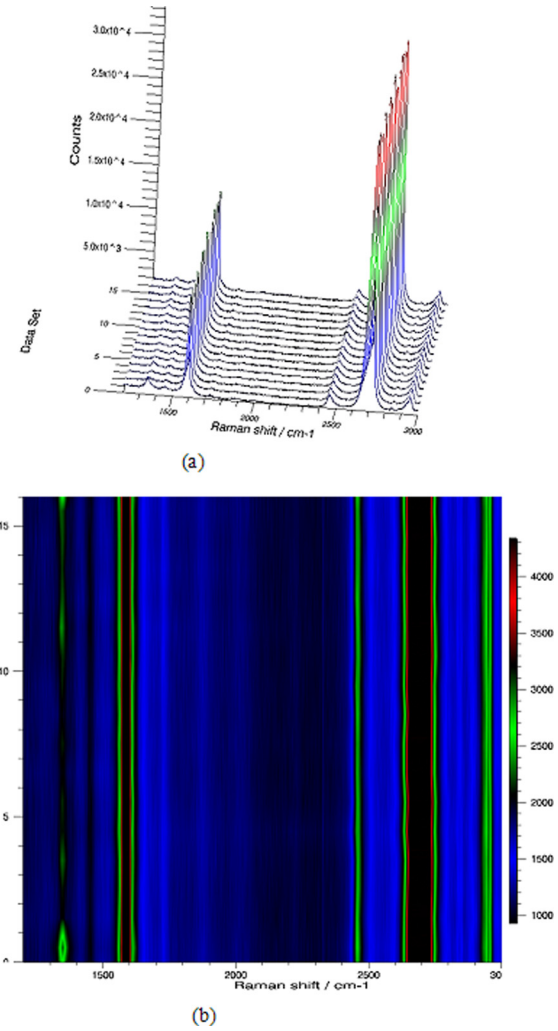

FIG. 2. (a) 3D Raman map of CVD grown graphene transferred on Si/SiO_2 substrates. Mapping step used was 4 μm. (b) 2D Raman map of CVD grown graphene transferred on Si/SiO_2 substrates. Mapping step used was 4 μm.

Raman system with 2400 line/mm grating, 514.5 nm excitation, and low level power (<2 mW) to avoid any heating effects. The Raman spectra were fitted with Voight function. The Raman mapping was done using a 4 μm step. Figs. 2(a) and 2(b) show the 3D and 2D representation of Raman mapping of CVD single-layer graphene. The results presented in these figures show that the CVD graphene is of good quality and has a low number of defects. The ratio I_{2D}/I_G that is used as a figure of merit for the graphene monolayer quality is between 2.73 and 2.86 and the ratio I_G/I_D is 3, and this is indicative of the presence of low density of defects. However, the surface of the antenna is large and we do not have a single graphene monolayer covering the entire area of the rectangular patch. On the contrary, it is known that hundreds of surface steps containing multilayer graphene and grains boundaries are present around islands of graphene monolayers with diameters of 5–20 μm. The technological process flow is simple, involving two main steps: (i) graphene patterning done by RIE etching and (ii) gold deposition followed by a lift-off process. Optical UV lithography was used. Typical edge roughness is <100 nm, which is orders of magnitude below the minimum features related to microwaves frequencies.

We measured the reflection parameter ($|S11|$) as a function of frequency (f) for the graphene-based antenna from Fig. 1 using an on-wafer probe station linked to an Anritsu-37397D Vector Network Analyzer (VNA). The SOLT (Short, Open, Load and Thru) calibration was performed to calibrate the VNA before measurements. A CS-5 standard CPW calibration kit was used. The graphene-based antenna is DC biased using the probe station ground-signal-ground (G-S-G) probe tips. So, the DC voltage is applied between the central conductor and the grounds of the CPW using the internal bias tee of the VNA coupled to a Keithley 4200-SCS (Semiconductor Characterization System) able to provide controllable voltage/current sources. The antenna is fixed on a metallic plate playing the role of a backside metallization. The results are displayed in Fig. 3 for X band.

We see an overall reflection loss of about −9 dB and two resonances located at 8.8 GHz and 11.4 GHz, corresponding to $|S11|$ minimum values of − 12.2 dB and −13.4 dB, respectively, at 0 V applied DC bias (solid black trace in Fig. 3). We see that the entire S11 dependence on frequency is shifted up and down depending on the applied voltages, while the resonances are shifted left or right with about 24 MHz. This is due to the fact that the surface resistance of the antenna is

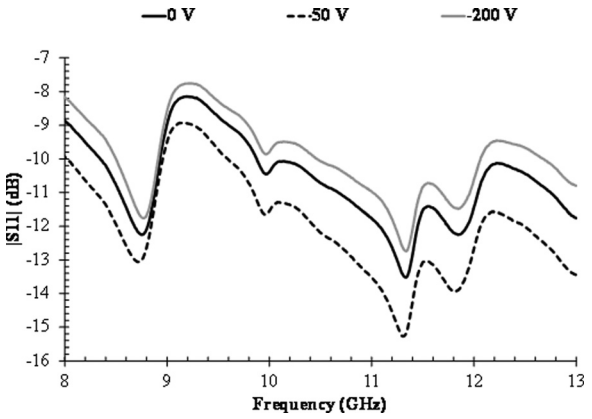

FIG. 3. $|S11|(f)$ in X band for three different bias voltages: 0 V (solid black trace), 50 V (dashed trace), and −200 V (solid grey trace).

decreasing at 50 V and, respectively, increasing at −200 V. We see that, at 11.4 GHz, when the surface resistance is decreasing, the matching of antenna is improving with 1.5 dB while when the surface resistance is increasing we lose about 0.4 dB. The large values of the DC applied voltage are due to the fact that the slot widths are rather large: 350 μm on x-axis and 600 μm on y-axis (see Fig. 1(c)), and so the field applied between the graphene patch and the coplanar ground is rather small. In order to understand the behavior of the graphene-based antenna described above, we use the equivalent circuit from Fig. 4(a), which was analyzed with AWR Microwave Office. The equivalent circuit is an R–L-C series circuit, where $R = R_s$ is the graphene's surface resistance and $L = L_s = L_k$ is graphene surface kinetic inductance. According to Ref. 18, in the unbiased case $L_k = 0.3$ nH, which corresponds to a reactance at 10 GHz equal to $X_s = \omega L_s = 19\,\Omega$. Further, R_s is 120 Ω, for unbiased case, and $C = 1.104$ pF is the total calculated capacitance between graphene and the underlying metallic surface used for measurements. A CPW transmission line with the length of 9.55 mm and gap-signal-gap of 50–100-50 μm (with a characteristic impedance of 50 Ω) is used to feed the antenna and inserted as a component in the equivalent circuit from Fig. 4(a). The metal thickness is 400 nm, and the thickness of the dielectric substrate is 500 μm. In Figs. 4(b) and 4(c), we have displayed the measured and simulated input impedance and the S11, and we see that the experimental results fit quite well with simulated results. From these latter curves, we can extract more precisely the impedances corresponding to the resonances of S11 (they are represented on the Smith chart by closed loops towards the center of the diagram). We have the first resonance at 8.748 GHz ($|S11| = -12.24$ dB), corresponding on Smith chart to R = 31.56 Ω and X = −7.734 Ω, and the second resonance

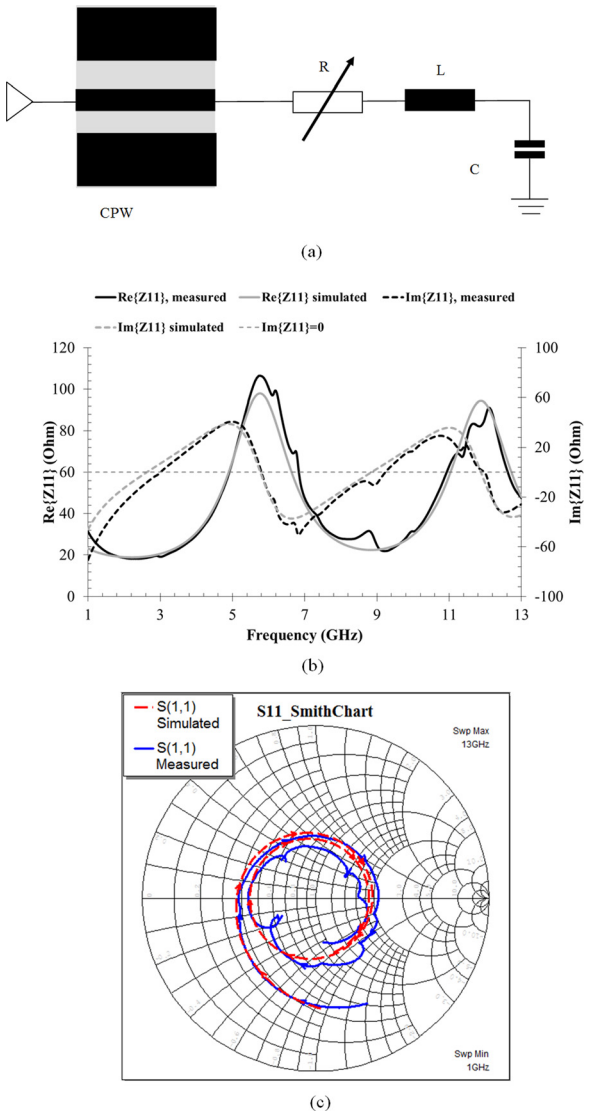

FIG. 4. (a) The equivalent circuit of the graphene antenna, (b) the measured and the simulated input impedance of the antenna, and (c) the measured and the simulated S11 represented on the Smith Chart at 0 V.

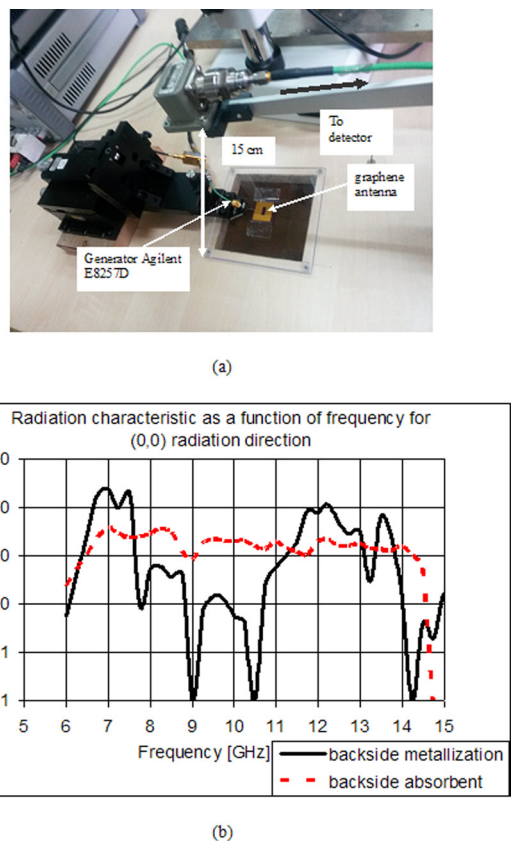

FIG. 5. (a) the radiation pattern measurement setup, (b) the detected signal as a function of frequency for the radiation direction normal to the antenna plane for a backside absorbent (dashed trace) and a backside metallization (solid trace).

located at 11.34 GHz ($|S11| = -13.51$ dB), corresponding on the Smith chart to $R = 67.57\,\Omega$ and $X = 17.91\,\Omega$. We see that the matching is not perfect but could be improved easily, since the reactive part is small, and the real parts are not far located from 50 Ω. The matching can be further improved with a more complex matching network.

The radiation pattern of the graphene-based antenna was measured using the setup from Fig. 5(a). The antenna under test was contacted on wafer with a G-S-G probe and used as emitter. It was fed by a PSG Analog Signal Generator (Agilent E8257C) with a 6–15 GHz microwave signal, modulated in amplitude (10 kHz square AM). A X-band waveguide flange was placed at a distance of 150 mm (satisfying far-field conditions in the X-band) and connected to a 10 MHz–40 GHz detector (Anritsu). The detected signal is amplified by a SR560 LNA and plotted on an oscilloscope (Tektronix DPO2024). Since the antenna has a thickness of 500 μm, much smaller than the microwave radiation wavelengths, which are of the order of few cm at least, the antenna will not only radiate above the radiation plane represented by slots but also below, thus reducing the radiation efficiency. So, we have measured the detected signal at the position (0,0)—perpendicular to the metallization—in two conditions: (i) placing a microwave absorbent on the backside of the antenna and (ii) placing metallic surface on the

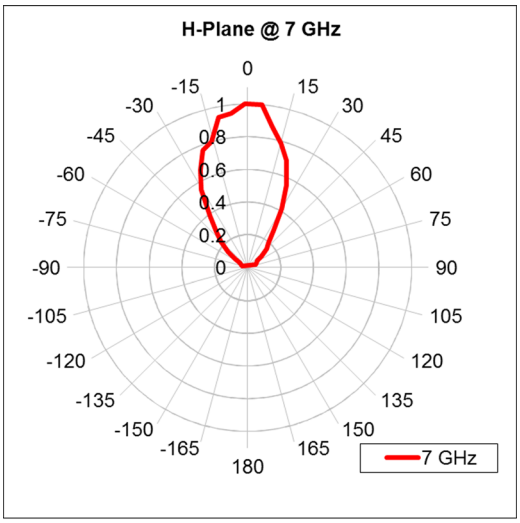

(a)

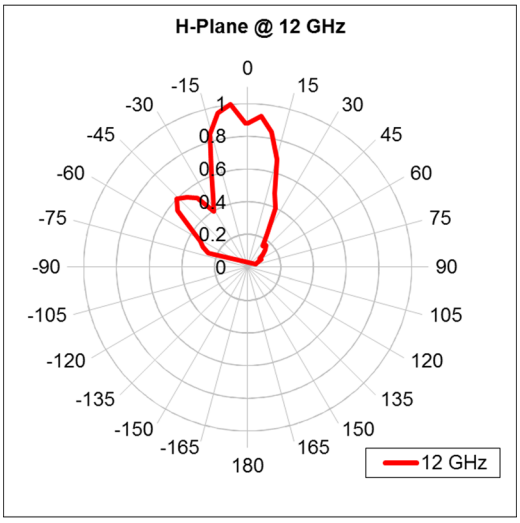

(b)

FIG. 6. The radiation pattern of the graphene-based antenna with a backside metallization normalized at the maximum value at (a) 7 GHz and (b) 12 GHz.

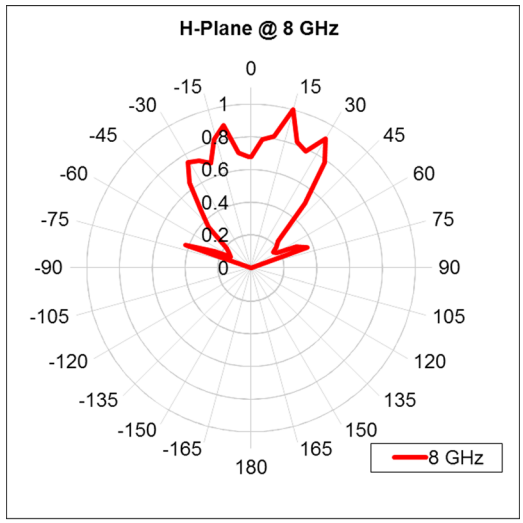

(a)

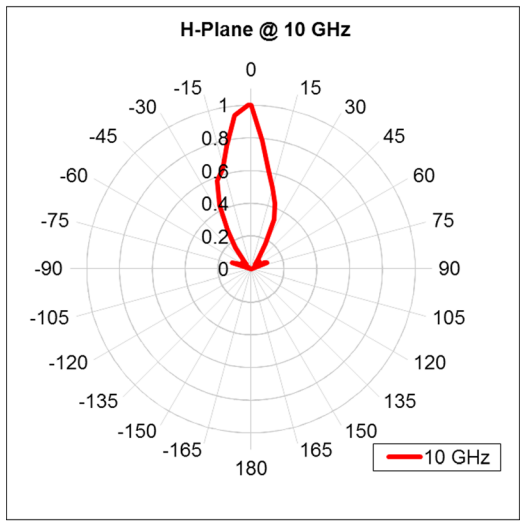

(b)

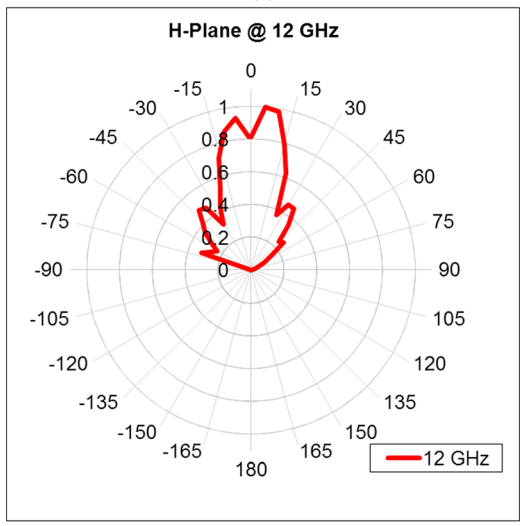

(c)

FIG. 7. The radiation pattern of the graphene-based antenna with a backside microwave absorbent normalized at the maximum value, at (a) 8 GHz, (b) 10 GHz, and (c) 12 GHz.

backside of the antenna. We can see in Fig. 5(b) that the detected signal in the case the backside metallization is much larger at 7 GHz and 12 GHz, while the detected signal in the case of the backside microwave absorbent is more uniform. The 2D radiation patterns in the H-plane (orthogonal to the feed line of the antenna) were recorded at 7 GHz and 12 GHz in the case of the graphene-based antenna with a backside metallized surface (see Fig. 6), and at 8 GHz, 10 GHz, and 12 GHz in the case of the graphene-based antenna with a backside absorbent (see Fig. 7). The 3 dB beamwidth (when the received power is reduced by half compared to the maximum) is between 40° and 80° for the radiation patterns presented in Figs. 6 and 7. In the case of the graphene-based antenna having a backside metallization, there are no side lobes at 7 GHz with one side lobe appearing at 12 GHz, meaning that part of the radiated microwave signal travels through the substrate towards the backside metallization and is then reflected back, being added with the frontside radiated signal. For the backside absorbent case, although the effects of the backside radiation are strongly diminished, multiple side lobes appear at 8 GHz and 12 GHz. The simulated gain of the antenna is −8 dB without backside metallization and −6 dB with backside metallization at 10 GHz. No calibrated gain measurements could be performed with the available equipment (see Fig. 5(a)). The radiation efficiency and gain are weak but can be improved by reducing the sheet resistance of graphene. This can be achieved by optimizing the technological process and the antenna topology, including the graphene DC bias configuration. In our case, we have biased graphene with a DC electric field via coplanar configuration so the electric field is tangential to the graphene surface. In conclusion, we have shown that a graphene-based antenna has unusual properties: the reflection parameter (|S11|) of the antenna is shifted up and down by the DC voltage improving the matching and, in contrast with metallic slot or patch antenna working at the same frequencies, the graphene-based antenna is wideband. This is due to graphene, which in microwave can be seen as variable resistor independent of frequency as it was initially shown in Ref. 16. Although there are some papers treating the simulations of microwave graphene antennas, published especially in various IEEE conferences (for example, Refs. 19 and 20), this letter presents a fully experimentally characterized microwave graphene-based antenna. The main applications of this antenna are RF communication, where due to its inherent tunability, the graphene antenna is able to work or switch on various channels in microwaves and microwave electromagnetic field sensing. The first application is similar to beamforming of the phased arrays,[21] and the second is similar to Ref. 22, both in the photonic domain.

We thank the European Commission for the financial support via the FP 7 NANO RF (Grant Agreement No. 318352).

[1]D. L. Sounas, H. S. Skulason, H. V. Nguyen, A. Guermoune, M. Siaj, T. Szkopek, and C. Caloz, "Faraday rotation in magnetically biased graphene at microwave frequencies," Appl. Phys. Lett. **102**, 191901 (2013).

[2]A. Drabińska, A. Wołoś, M. Kamińska, W. Strupinski, and J. M. Baranowski, "Microwave studies of weak localization and antilocalization in epitaxial graphene," AIP Conf. Proc. **1566**, 159 (2013).

[3]X. Song, M. Oksanen, J. Li, P. J. Hakonen, and M. A. Sillanpää, "Graphene optomechanics realized at microwave frequencies," Phys. Rev. Lett. **113**, 027404 (2014).

[4]V. Singh, S. J. Bosman, B. H. Schneider, Y. M. Blanter, A. Castellanos-Gomez, and G. A. Steele, "Optomechanical coupling between a multilayer graphene mechanical resonator and a superconducting microwave cavity," Nat. Nanotechnol. **9**, 820–824 (2014).

[5]P. Jiang, A. F. Young, W. Chang, P. Kim, L. W. Engel, and D. C. Tsui, "Quantum oscillations observed in graphene at microwave frequencies," Appl. Phys. Lett. **97**, 062113 (2010).

[6]D. Dragoman and M. Dragoman, "Time flow in graphene and its implications on the cutoff frequency of ballistic graphene devices," J. Appl. Phys. **110**, 014302 (2011).

[7]Z. Guo, R. Dong, P. Sarathi Chakraborty, N. Lourenco, J. Palmer, Y. Hu, M. Ruan, J. Hankinson, J. Kunc, J. D. Cressler, C. Berger, and Walt A. de Heer, "Record maximum oscillation frequency in c-face epitaxial graphene transistors," Nano Lett. **13**, 942–947 (2013).

[8]L. Liao, J. Bai, R. Cheng, Y.-C. Lin, S. Jiang, Y. Qu, Y. Huang, and X. Duan, "Sub-100 nm channel length graphene transistors," Nano Lett. **10**, 3952–3956 (2010).

[9]M. Dragoman, A. Dinescu, and D. Dragoman, "Negative differential resistance in graphene based ballistic field-effect transistor with oblique top gate," Nanotechnology **25**, 415201 (2014).

[10]M. Dragoman, D. Neculoiu, G. Deligeorgis, G. Konstantinidis, D. Dragoman, A. Cismaru, A. A. Muller, and R. Plana, "Millimeter-wave generation via frequency multiplication in graphene," Appl. Phys. Lett. **97**, 093101 (2010).

[11]S.-J. Han, A. Valdes Garcia, S. Oida1, K. A. Jenkins, and W. Haensch, "Graphene radio frequency receiver integrated circuits," Nat. Commun. **5**, 3086 (2014).

[12]M. Dragoman, D. Neculoiu, A. Cismaru, G. Deligeorgis, G. Konstantinidis, and D. Dragoman, "Graphene radio: Detecting radiowaves with a single atom sheet," Appl. Phys. Lett. **101**, 033109 (2012).

[13]L. Vicarelli1, M. S. Vitiello, D. Coquillat, A. Lombardo, A. C. Ferrari, W. Knap, M. Polini, V. Pellegrini, and A. Tredicucci, "Graphene field-effect transistors as room-temperature terahertz detectors," Nat. Mater. **11**, 865–871 (2012).

[14]A. Zak, M. A. Andersson, M. Bauer, J. Matukas, A. Lisauskas, H. G. Roskos, and J. Stake, "Antenna-integrated 0.6 THz FET direct detectors based on CVD graphene," Nano Lett. **14**, 5834–5838 (2014).

[15]A. Zurutuza and C. Marinelli, "Challenges and opportunities in graphene commercialization," Nat. Nanotehnol. **9**, 730–734 (2014).

[16]M. Dragoman, D. Neculoiu, A. Cismaru, A. A. Muller, G. Deligeorgis, G. Konstantinidis, D. Dragoman, and R. Plana, "Coplanar waveguide on graphene in the range 40 MHz–110 GHz," Appl. Phys. Lett. **99**, 033112 (2011).

[17]A. Ahemed, I. A. Godthorpe, and A. K. Khandani, "Electrically tunable materials for microwave applications," Appl. Phys. Rev. **2**, 011302 (2015).

[18]H. Yoon, C. Forsythe, L. Wang, N. Tombros, K. Watanabe, T. Taniguchi, J. Hone, P. Kim, and D. Ham, "Measurement of collective dynamical mass of Dirac fermions in graphene," Nat. Nanotechnol. Lett. **9**, 594–599 (2014).

[19]J. Perruisseau-Carrier, "Graphene for antenna applications: Opportunities and challenges from microwaves to THz," in *Loughborough Antennas and Propagation Conference (LAPC)* (IEEE, 2012), pp. 1– 4.

[20]J. Perruisseau-Carrier, M. Tamagnone, J. S. Gomez-Diaz, and E. Carrasco, "Graphene antennas: Can integration and reconfigurability compensate for the loss?," in *European Microwave Conference (EuMC)* (IEEE, 2013), pp. 369–372.

[21]M. Burla, D. A. I. Marpaung, Z. Leimeng, M. R. Khan, A. Leinse, W. Beeker, M. Hoekmanm, R. G. Heideman, and C. G. H. Roeloffzen, "Multiwavelength-integrated optical beamformer based on wavelength division multiplexing for 2-D phased array antennas," J. Lightwave Technol. **32**(20), 3509–3520 (2014).

[22]X. Zhang, A. Hosseini, H. Subbaraman, W. Shiyi, Z. Qiwen, L. Jingdong, A. K.-Y. Jen, and R. T. Chen, "Integrated photonic electromagnetic field sensor based on broadband bowtie antenna coupled silicon organic hybrid modulator," J. Lightwave Technol. **32**(20), 3774–3784 (2014).